Insertion of Externally Administered Amyloid β Peptide 25−35 and Perturbation of Lipid Bilayers[†]

Silvia Dante,*[,‡,§] Thomas Hauss,[§,||] and Norbert A. Dencher[‡]

Physical Biochemistry, Darmstadt University of Technology, Petersenstrasse 22, D-64287 Darmstadt, Germany, Institute of Physical Biology, Heinrich-Heine-Universität, D-40225 Düsseldorf, Germany, and BENSC, Hahn-Meitner-Institut, Glienicker Strasse 100, D-14109 Berlin, Germany

Received June 18, 2003; Revised Manuscript Received September 23, 2003

ABSTRACT: To understand the molecular basis and to prevent diseases such as Alzheimer's disease (AD), the targets of the triggering agent have to be elucidated. β-Amyloid peptide (Aβ) is the major component of extracellular senile plaques characteristic of AD. For a very long time, the aggregated form of the Aβ was supposed to be responsible for the neurodegeneration that occurs in AD. Recently, the attention has been diverted to the monomeric or oligomeric forms of Aβ and their interaction with cellular targets. In our investigation, the physiological and medically important insertion of externally applied Aβ monomers into the bilayer of lipid vesicles is demonstrated. Aβ(25−35) has been localized in the region of the lipid alkyl chain, and it has a severe disordering effect on the lamellar order of the lipid bilayer. Both of these results are of biomedical relevance.

Alzheimer's disease (AD)[1] is characterized by the formation of amyloid plaques, deposited in the neuronal extracellular space of the brain and surrounded by dystrophic neurons. The major component of these aggregates is Aβ, a 39−42 amino acid peptide produced by enzymatic cleavage of a 770 amino acid membrane spanning precursor protein. The so-called amyloid hypothesis links the presence of the insoluble fibril-like Aβ aggregates to the pathogenesis of the disease. For more than a decade the amyloid hypothesis has been the driving idea in the attempt to understand the trigger of the neuritic damage leading to dementia. A huge amount of data has been collected, in vivo and in vitro, that supports this theory; evidence in favor of it are for instance the death of neurons after administration of Aβ (*1*−*3*) and the observation of neurotoxicity of the fibrillar form of Aβ after intracerebral injection (*4*, *5*). Other experimental evidence has been collected which does not support the assumption of neurotoxicity of fibrillar Aβ. For instance, transgenic mice that accumulate a big load of plaques containing fibrillar Aβ, show no or little neurotoxic response to this load (*6*). Other results were equivocal or not reproducible, this fact being ascribed to methodological differences (*2*, *3*, *7*, *8*). Recently, new suppositions have been put forward. In a very provocative article (*9*) Bishop and Robinson highlighted the weakness of the amyloid hypothesis and suggested that Aβ might have a neuroprotective role instead (bioflocculant hypothesis). Other studies focus on nonfibrillar, shorter soluble forms of monomeric or dimeric Aβ and show that they can be highly toxic. A strong correlation of the neurodegenerative process with the absolute level of soluble amyloid has been found (*6*). Moreover, soluble forms of Aβ may be released from the senile mature plaques, interact with the neurons, and cause neuron damage or disruption (*10*). In this scenario, it is relevant to identify the target (e.g., a specific receptor or organelle or the lipid membrane itself) of Aβ. It is also pertinent to investigate the interaction of monomeric Aβ with lipid membranes, to clarify its possibility to intercalate in the lipid core, and to identify its location in the membrane. Very few direct methods have been applied for this purpose in the past. In this work, we have applied neutron diffraction in conjunction with selective amino acid deuteration to localize a short fragment of Aβ, namely, Aβ(25−35), in small unilamellar vesicles. Aβ(25−35) (GSNKGAIIGLM) is considered to be the reactive part of Aβ(1−42), since it shows fibrillogenic activity and has a neurotoxic effect on cultured cells. Aβ(25−35) has channel-forming activity in bilayers (*11*). It was found to alter membrane fluidity in rat brain and in human cortex membranes (*12*, *13*) and to modulate membrane lipid peroxidation (*14*). Its interaction with lipid layers has been studied with a variety of biochemical techniques, and it was described to be dependent on the membrane composition, on the aggregation state of the peptide, and on pH and ionic strength (*15*−*18*).

In previous papers the location of Aβ(25−35) in oriented lipid bilayer samples was investigated by diffraction techniques, and the presence of the peptide in the hydrophobic core of the membrane was established (*19*−*21*). In the present study, for the first time we were able to prove by

[†] This work was supported by Grant 03-DEE8DA from Bundesministerium für Bildung und Forschung, by the Fonds der Chemischen Industrie (to N.A.D.), and by the Research Center Jülich (F+E).

* Corresponding author. E-mail: silvia.dante@hmi.de. Tel: +49 30 8062 2071. Fax: +49 30 8062 2999.

[‡] Darmstadt University of Technology.

[§] Hahn-Meitner-Institut.

[||] Heinrich-Heine-Universität.

[1] Abbreviations: Aβ(25−35), β-amyloid (25−35); AD, Alzheimer's disease; POPC, 1-palmitoyl-2-oleoylphosphatidylcholine; POPS, 1-palmitoyl-2-oleoylphosphatidylserine; TFA, trifluoroacetic acid; rh, relative humidity; H-Leu34-Aβ(25−35), β-amyloid (25−35) with protonated leucine in position 34; ^{2}H-Leu34-Aβ(25−35), β-amyloid (25−35) with deuterated leucine in position 34; fwhm, full width at half-maximum.

10.1021/bi035056v CCC: $25.00
Published on Web 10/30/2003

neutron diffraction the penetration of Aβ(25−35) and to determine the depth of penetration of the C-terminus in the bilayer core when Aβ(25−35) was externally administered. Neutron diffraction is indeed a sensitive and direct method for delineating the structure of the bilayer profile. In the study of biological samples, the advantage of neutron diffraction is based on the large difference in the scattering length of hydrogen ($b_H = -0.37 \times 10^{-14}$ m) and deuterium ($b_D = 0.67 \times 10^{-14}$ m). Using the isomorphous replacement technique it is therefore possible to locate, with high sensitivity and without perturbing the system, a selectively deuterated part of a molecule in a structure even at lower spatial resolution (*22*, *23*). In the present study the penultimate amino acid in the C-terminal region of Aβ(25−35), a leucine containing 10 hydrogens, was selectively deuterated. Diffraction patterns obtained from lipid samples containing the deuterated and the protonated species of Aβ(25−35), respectively, were compared. A mixture of 92:8 mol/mol of 1-palmitoyl-2-oleoylphosphatidylcholine (POPC) and 1-palmitoyl-2-oleoylphosphatidylserine (POPS) was used to mimic, as closely as possible, the composition and the negative charge state of neuritic cell membranes without increasing the complexity of the system too much.

The fundamental difference in comparison with previous studies of Mason and co-workers (*19*, *20*) and of our own group (*21*) is that Aβ(25−35) was provided to the lipid vesicles from the external aqueous solution, and the spontaneous insertion of the peptide in the membrane was investigated. The localization of the deuterated Aβ(25−35) and the perturbation of the structure of the lipid bilayers upon membrane insertion could be demonstrated.

MATERIALS AND METHODS

Sample Preparation. 1-Palmitoyl-2-oleoylphosphatidylcholine (POPC) and the net negatively charged lipid 1-palmitoyl-2-oleoylphosphatidylserine (POPS) were purchased from Avanti Polar Lipids (Alabaster, AL). The lipids were cosolubilized in chloroform in a ratio of 92:8 mol/mol POPC/POPS; after evaporation of the solvent under a nitrogen stream, the lipids were desiccated under vacuum ($p < 1$ mbar) for 12 h and redispersed in ultrapure water (Millipore) in a concentration of 0.5 mg/mL. Small unilamellar vesicles were obtained by sonication in an ultrasonic bath, until a translucent lipid dispersion was obtained. The same vesicle suspension was used for the preparation of the three samples under investigation.

Aβ(25−35) peptide (GSNKGAIIGLM) was synthesized and purified to 95% by WITA GmbH (Teltow, Germany). Two batches of the peptide were prepared, one protonated and one containing a deuterated leucine (10 deuterons) at position 34, i.e., the penultimate amino acid. To avoid preaggregation, a pretreatment with trifluoroacetic acid (TFA, by Sigma) (*24*) was applied. The peptide−TFA solution was dried in a quartz tube under a stream of nitrogen and put under vacuum ($p < 1$ mbar) for 12 h to remove all traces of TFA. The peptides were then dissolved in ultrapure water (concentration 0.43 mg/mL) and immediately added to the vesicles. The incubation of the peptide was carried out by adding aliquots (50 μL) of the peptide solutions to the vesicles while a short sonication burst of 2 s was applied by a bath type sonicator, to mix the sample and increase the diffusion of the peptide. The time interval between the additions of two successive drops was at least 15 min.

Oriented samples were obtained by spreading the aqueous dispersions onto quartz slides (65 mm × 15 mm × 0.3 mm) and allowing them to dry for 24 h at room relative humidity (rh) and temperature in a dust-free environment. The samples were rehydrated at 25 °C in an atmosphere of 98% rh maintained with a saturated salt solution (K_2SO_4).

Each sample contained 20 mg of lipids and 3 mol % peptide, either perprotonated or selectively deuterated to have a sample with Aβ concentration as low as possible, compatible with the signal detection. A control sample, containing only the lipid mixture, was also prepared.

Neutron Diffraction and Data Analysis. Neutron diffraction measurements were carried out on the membrane diffractometer V1 at the Berlin Neutron Scattering Center of the Hahn-Meitner-Institut, Berlin, Germany. The procedure for the sample investigation is reported in detail elsewhere (*21*). Briefly, the samples were placed in an aluminum sample container, in which the temperature was controlled ($T = 27.0 \pm 0.1$ °C) for all samples and the humidity adjusted by aqueous saturated solutions of K_2SO_4 kept in Teflon water baths. Contrast variation was achieved by adjusting the atmosphere in the sample container to four different compositions of D_2O:H_2O (i.e., 50:50, 20:80, 8:92, and 0:100). After each change of the aqueous solution, the samples were left to equilibrate for 24 h.

Samples were vertically mounted, and diffraction intensities were measured with rocking scans, rocking the sample around the expected Bragg position θ by $\theta \pm 2°$. The duration of each rocking scan varied from 20 min to 4 h depending on the intensity of the reflection. Diffraction patterns of POPC/POPS bilayers, of POPC/POPS bilayers containing 3% (mol) ^{2}H-Leu34-Aβ(25−35), and of POPC/POPS containing 3% (mol) H-Leu34-Aβ(25−35) were measured. The lamellar spacing d of each sample was calculated by least-squares fitting of the observed 2θ values to the Bragg equation $n\lambda = 2d \sin(\theta)$, where n is the diffraction order and λ is the selected neutron wavelength (4.52 Å). Integrated intensities were calculated with Gaussian fits to the experimental Bragg reflections. Intensities, corrected with absorption and Lorentz factors, were square rooted to produce the structure factor amplitudes $F(h)$. The relative absolute density profile $\rho(z)$ is given by

$$\rho(z) = \rho_0 + \frac{2}{d}\sum_{h=1}^{n} F(h) \cos\left(\frac{2\pi h z}{d}\right) \qquad (1)$$

where F is in units of scattering length and ρ_0 is the average scattering length per unity length of the bilayer, $F(h)$ are the scaled structure factors, and the sum describes the distribution in scattering lengths across the bilayer.

The phase assignment was obtained with the isomorphous replacement method, using the D_2O:H_2O exchange, where the structure factors are a linear function of the mole fraction of D_2O:H_2O (*25*). Structure factors at four different isotopic water vapor compositions were measured for each sample. For any further data evaluation, i.e., for the localization of the label, only the structure factors obtained at 8% D_2O, where the scattering length density of the water layer is zero, were employed. It is not appropriate to use the structure

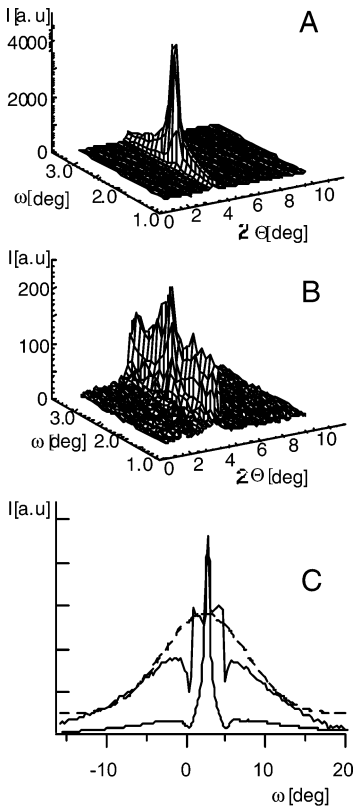

FIGURE 1: Rocking curves obtained by rotating the samples around the first Bragg peak ($2\theta = 4.57$) of an angle $\omega = \pm 2°$. In the case of the pure lipid membrane a narrow, intense peak centered at $\omega = 2.28°$ is obtained (panel A), indicating a well-aligned sample. In the case of the vesicle incubated with Aβ(25−35) (panel B), the sample is powder-like, and the diffracted intensity is spread to a wide angular range. Long rocking curves (±20°), integrated in the 2θ range, of the samples with (solid line) and without Aβ(25−35) (dotted line) and measured in 100% D_2O atmosphere are compared in panel C. For clarity, the curves are arbitrarily scaled to the maximal intensity. The broadening of the rocking curve in the presence of the peptide is evident. The dashed line is the Gaussian fit of the broad mosaicity with a fwhm = 8.5°. A narrow peak at the Bragg position is still visible in the sample containing Aβ(25−35). The two dips in the experimental curves at 0 and 4.57° are due to the absorption by the samples of the direct and diffracted neutron beam, respectively.

factors at 100% or 50% D_2O to determine the label position via the Fourier difference method. At these contrasts the large coherent scattering of the water layer hides that of the membrane. The difference in coherent scattering length due to the labeled Aβ is reduced to 1.3% only compared to 13.8% in 100% H_2O and becomes barely detectable. The position of the deuterated amino acid was determined by the differences of the densities between samples with Aβ containing deuterated and protonated leucine on a relative scale. The distribution of the label is fitted in reciprocal space to the position and amplitude of a Gauss function using the measured structure factors up to the fifth order.

RESULTS AND DISCUSSION

Figure 1 depicts the rocking curves around the first Bragg reflex of two samples, in the absence (Figure 1A) and in the presence (Figure 1B) of Aβ(25−35). In the first case, a mosaicity (i.e., a distribution of the membrane orientation with respect to the quartz support) inferior to 0.5° demonstrates the very good quality of the sample; the narrow peak centered at $2\theta = 4.57$ is due to the long-range lamellar order of the lipid bilayers, while the wings of the peak are due to the portion of the sample, in this case a small one, that has a less ordered (i.e., powder-like) arrangement. For a pure lipid sample this mosaicity is routinely achieved for oriented planar membrane stacks (see, e.g., refs *26* and *27*).

The rocking curve is very different when Aβ(25−35) has been incubated with the vesicles. The lattice orientation of the sample is heavily perturbed and spread in a powder-like form. This results in a dramatic decrease of the Bragg peak intensity, as shown in Figure 1B (note the expanded ordinate scale), due to the fact that the scattered intensity is spread over a wide angular range. Figure 1C shows a long rocking curve (±20°) around the first Bragg peak (solid line) of the sample containing Aβ(25−35). A broad Gaussian distribution (fwhm = 8.5°) describes the lattice disorientation generated by the peptide. A region with narrower mosaicity is still visible at the Bragg position; as a comparison, a rocking curve of the sample without Aβ(25−35) is reported (dotted line), showing the narrow mosaicity of 0.5° fwhm. Oligomers and aggregates potentially formed by the peptide in solution when applied to the vesicle dispersion may be a source for the lattice disorder, since they could hinder a planar stacking of the lipid bilayers if the membranes fold around them. Alternatively, and biomedically more relevant, it is possible that the incorporated Aβ(25−35) alters the physical state of the membrane, for instance, inducing lipid domain formation (*28*) or even rupture of the lipid bilayers (*29*) causing the misalignment of the membranes. We like to point out that we have never observed this effect when studying a different system in which the peptide has been applied to the lipid solution before forming the oriented lipid bilayers. In that case, the mosaicity of the samples was even narrower than that shown in Figure 1A, and the presence of the peptide caused no difference. That preparation method was hampered by the fact of being not physiological because of the solvent employed and because the peptide did not interact with the lipid from the outside of the bilayer but was "built in" in the lipid bilayers.

Despite the disordering effect of the peptide, at least up to 5 orders of diffraction was detectable in all samples. Due to the limited beam time available, the sample investigation was constrained to 5 orders even for those samples (i.e., the pure POPC/POPS samples) where, in principle, more orders could have been detected.

In Figure 2 an example of the obtained diffraction patterns, corresponding to the spectra of the three different samples in the same H_2O:D_2O contrast, i.e., 80:20, is reported. The diffraction patterns show up to 5 lamellar orders. The lamellar spacing d of each sample was calculated by least-squares fitting of the observed 2θ values to the Bragg equation $n\lambda = 2d \sin(\theta)$, where n is the diffraction order and λ is the selected neutron wavelength (4.52 Å). The repeat distance of all three samples was not significantly different, i.e., $d = 54.2 \pm 0.4$ Å for the POPC/POPS sample and $d = 54.4 \pm 0.4$ Å for the samples containing Aβ(25−35) in the protonated and deuterated forms, respectively, indicating that the membrane thickness and hydration are not affected by the peptide. In Figure 2 differences in the ratio between the peak intensities are visible, considering both the sample with and without peptide and the sample with protonated and deuterated peptide. These differences translate in different structure

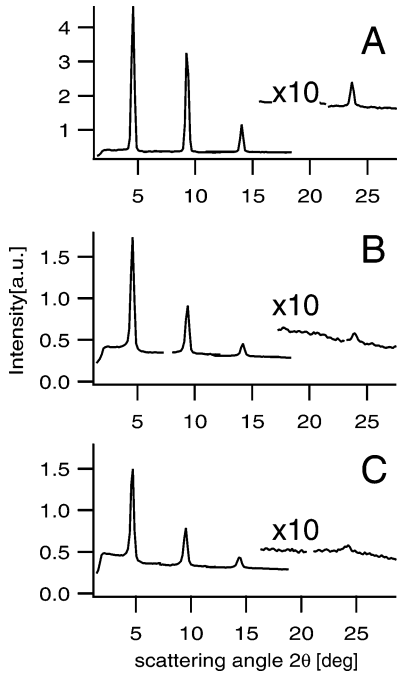

FIGURE 2: 2. Diffraction patterns of POPC/POPS bilayers (A), POPC/POPS incubated with H-Leu34-Aβ(25−35) (B), and POPC/POPS incubated with ^{2}H-Leu34-Aβ(25−35) (C) at 20% D_2O. Five orders of diffraction are visible for each sample, with different relative peak intensities. The intensity of the fourth diffraction order is nearly zero in all samples.

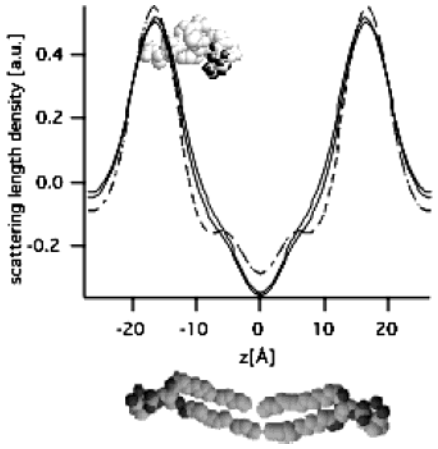

FIGURE 3: Scattering length density profiles at 8% D_2O in the direction normal to the membrane plane of the samples containing deuterated (solid line) and protonated (dotted line) Aβ(25−35). The profile of a pure lipid sample (dashed−dotted line) is shown as a reference. A sketch of the bilayer is shown below. In the upper part of the diagram, a sketch of the peptide is reported. The structural model is obtained from ref *30*. The deuterons of the labeled leucine are colored gray. As reported in the text, no direct information about the orientation of the peptide in the lipid bilayers is obtained from our results. Nevertheless, the sketched orientation of the peptide is suggested by thermodynamic considerations.

factor sets in reciprocal space and, after the calculation of the Fourier transformation, result in different scattering length density profiles of the respective membranes in the direction perpendicular to the membrane plane reflecting the label position, i.e., the localization of Leu34 as well as the Aβ-induced changes in the structure of the lipid bilayer. The calculated profiles are displayed in Figure 3. As depicted in the sketch at the bottom illustrating the orientation of the lipid bilayer, the water region is at the edges of the figure;

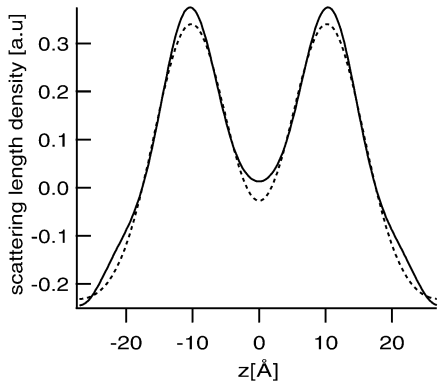

FIGURE 4: Difference scattering length density profile between the samples with deuterated and protonated Aβ(25−35) (solid line) and its fit to a Gaussian distribution (dotted line) truncated to the fifth Fourier term.

the two maxima of the scattering length density represent the polar headgroups of the lipids, and the trough in the middle corresponds to the terminal methyl groups of the lipid chains. In fact, due to the negative scattering length of hydrogen, the regions of the unit cell rich in hydrogen give a more negative signal. Comparing the profiles of samples with and without Aβ, it is straightforward that the presence of the peptide induces a notable modification of the scattering length density profile. In particular, the polar head region is broadened, and the inner part of the membrane is heavily perturbed. Smaller, but significant, differences between the profiles of POPC/POPS containing protonated or deuterated Aβ(25−35) also exist. This difference is outside the confidence limit (data not shown); the significance of the difference between the two profiles is also confirmed by the fact that independent measurements of membranes with identical composition produce scattering length density profiles that are perfectly superimposable (data not shown). Moreover, differences between the profile of lipid bilayers containing H-Leu34-Aβ(25−35) and ^{2}H-Leu34-Aβ(25−35) at each of the four measured D_2O:H_2O contrasts exhibit differences exactly in the same region of the unit cell.

The information about the location of the deuterated Leu34 originates from the difference between the membrane profiles of the sample containing ^{2}H-Leu34-Aβ(25−35) and the sample containing H-Leu34-Aβ(25−35). The corresponding scattering length density profile is reported in Figure 4. The experimental difference between the two scattering length density profiles was modeled and fitted to a Gaussian distribution of the label (and its mirror image in the centrosymmetric unit cell). The fitting process was carried out in the reciprocal space, comparing the calculated structure factors of the model with the observed structure factor differences between the sample containing ^{2}H-Leu34-Aβ-(25−35) and the sample containing H-Leu34-Aβ(25−35). Variables of the fit were height, position, and width of the Gaussian function. The comparison of the fitted difference density to the experimental difference density is shown in Figure 4. The deuterium distribution is located inside the membrane core at $|z| = 10.2 \pm 1.0$ Å from the center of the cell. This is in good agreement with our previous work (*21*), as discussed later, where we found that Aβ(25−35) initially intermixed with the lipids in organic solvent was intercalated in the hydrocarbon core of a lipid bilayer at a position close to the double bond of the unsaturated lipid chain (i.e., $|z| =$

5.9 ± 1.0 Å). The full width at half-maximum of the Gaussian distribution is 5 Å in the present experiment, compared to 2.85 Å in the previous study. This means that in this study the Aβ peptide has a broader distribution inside the membrane. A structural model of the peptide derived by Kohno et al. (*30*) and its possible location in the membrane are reported in Figure 3. The deuterons of the labeled leucine are colored gray. The current experiment does not provide an indication for the orientation of the peptide in the membrane, and the figure has to be considered as a guide for the eye.

In our previous investigation (*21*) two populations of the peptide had been detected, one inside the lipid bilayer and the second one in the water phase between the membranes. In the present experiment no deuterated label is detected in the water phase between the membranes. When the peptide is cosolubilized in chloroform with the lipids, as in the procedure employed in ref *21*, it has the possibility of depositing between each bilayer during the self-assembling of the membrane stacks, and it originates a coherent scattered signal. This coherence is absent in the experiment involving the vesicle, where Aβ(25−35) potentially aggregating in the aqueous solution is then randomly distributed in the dried sample and eventually distributed in the rehydrated membranes. The relative amount of the two populations and the depth of intercalation in the membrane core are a function of the lipid charge. In particular, in a zwitterionic POPC membrane, most of the deuterated label (86%) was found in the vicinity of the lipid headgroups (i.e., at $|z| = 14.3$ Å from the bilayer center), while in a charged POPC/POPS membrane, 54% of the deuterated leucine was localized in the vicinity of the hydrocarbon double bond, at $|z| = 5.9$ Å from the center. In the current investigation the deuterated label has also been localized in the hydrocarbon region at $|z| = 10.2$ Å from the center, slightly shifted with respect to the previous result in a membrane of nominally identical composition (i.e., 92:8 POPC/POPS). This finding points to the fact that the physical state of the membrane may influence greatly the location of the peptide. The sprayed samples previously investigated (*21*) result in planar membranes, while the interaction of the externally administered peptide with the lipids occurs with the outer leaflet of small unilamellar vesicles, with a diameter of about 50 nm and a high curvature. It is well documented that there are profound differences in the physical properties such as the surface tension between planar and highly curved lipid bilayers; these differences may lead to the moderately different positions of Leu34 in the membrane profile. We point out anyway that although the interaction of the peptide in the vesicle dispersion occurs only with the outer lipid layer, an asymmetry in the location of the label inside the bilayer cannot be detected by diffraction, since the results (i.e., the scattering length densities) reflect the central symmetry of the randomly stacked bilayers. A further variation between the methodological procedures applied in our two papers is that no interaction of Aβ(25−35) with organic solvent, such as chloroform, occurs at any step of the preparation involving vesicles.

The observation that Aβ(25−35) intercalates in the hydrocarbon region is supported by thermodynamic consideration. The thermodynamics of insertion of small peptides in lipid membranes has been investigated intensively by different groups (*31*−*36*), and it can follow different paths. The experimental determination of the total free energy of insertion is a rather difficult task. White and Wimley (*35*) suggest an "indirect" interfacial path of insertion consisting of the partitioning of the unfolded peptide from water to the interface, the folding in the interface, and the insertion of the folded peptide. A useful quantity to estimate is the free energy correlated to the unfolded peptide partitioning. According to the hydrophobicity scale (*35*) a total free energy of transfer of Aβ(25−35) from water to a lipid interface of +0.33 kcal/mol is calculated. Since negatively charged membranes have been used and Aβ(25−35) has a positively charged lysine residue in its sequence, an electrostatic attraction of the peptide by the membrane is anticipated but not a penetration. On the other hand, the molecule represents a strong hydrophobic dipole, meaning that the N-terminal segment GSNKGA is hydrophilic ($\Delta G = +1.73$ kcal/mol) and the C-terminus IIGLM is hydrophobic ($\Delta G = -1.4$ kcal/mol). The hydrophobic dipole would be even more enhanced if calculated according to Thorgeirsson et al. (*36*). Therefore, one can hypothesize that the C-terminal part of the peptide inserts in the membrane while the N-terminal part is located in the headgroup region of the membrane.

CONCLUSIONS

The findings of our investigation are of relevance for biomedical applications.

First, the externally administered Aβ(25−35) penetrates deeply into the lipid bilayers. This is the structural basis for the previously described channel-creating properties of Aβ (*11*, *37*). On the other hand, it may also interact with integral membrane proteins such as receptors. Furthermore, as exemplified by the broadening of the scattering density in the headgroup region and by the structural changes in the hydrophobic core (see Figure 3), the membrane is severely perturbed by the intercalated Aβ(25−35). This is the first direct structural proof for the previously observed perturbation of the membrane permeability induced by Aβ(25−35) (*11*, *37*).

Finally, we have evidence for a membrane disruption or domain formation induced by the Aβ peptide, as indicated by the increase in mosaicity of the membrane stacks (Figure 1). These changes in the supramolecular organization of the membrane may have a severe effect on the cell physiology. The membrane insertion of Aβ and the resulting structural defects will be of relevance for our understanding of AD and might promote a future pharmaceutical treatment.

ACKNOWLEDGMENT

We thank an anonymous referee for calling our attention to the thermodynamic properties of the amyloid peptide.

REFERENCES

1. Lorenzo, A., and Yankner, B. A. (1996) *Ann. N.Y. Acad. Sci. 777*, 89−95.
2. May, P. C., Gitter, B. D., Waters, D. C., Simmons, L. K., Becker, G. W., Small, J. S., and Robison, P. M. (1992) *Neurobiol. Aging 13*, 605−607.
3. Busciglio, J., Lorenzo, A., and Yankner, B. A. (1992) *Neurobiol. Aging 13*, 609−612.
4. Joachim, C. L., and Selkoe, D. J. (1992) *Alzheimer Dis. Assoc. Disord. 6*, 7−34.

5. Inoue, S., Kuroiwa, M., and Kisilevsky, R. (1999) *Brain Res. Brain Res. Rev. 29*, 218−231.
6. McLean, C. A., Cherny, R. A., Fraser, F. W., Fuller, S. J., Smith, M. J., Beyreuther, K., Bush, A. I., and Masters, C. L. (1999) *Ann. Neurol. 46*, 860−866.
7. Games, D., Khan, K. M., Soriano, F. G., Keim, P. S., Davis, D. L., Bryant, K., and Lieberburg, I. (1992) *Neurobiol. Aging 13*, 569−576.
8. Podlisny, M. B., Stephenson, D. T., Frosch, M. P., Lieberburg, I., Clemens, J. A., and Selkoe, D. J. (1992) *Neurobiol. Aging 13*, 561−567.
9. Bishop, G. M., and Robinson, S. R. (2002) *Neurobiol. Aging 23*, 1101−1105.
10. Lambert, M. P., Barlow, A. K., Chromy, B. A., Edwards, C., Freed, R., Liosatos, M., Morgan, T. E., Rozovsky, I., Trommer, B., Viola, K. L., Wals, P., Zhang, C., Finch, C. E., Krafft, G. A., and Klein, W. L. (1998) *Proc. Natl. Acad. Sci. U.S.A. 95*, 6448−6453.
11. Mirzabekov, T., Lin, M. C., Yuan, W. L., Marshall, P. J., Carman, M., Tomaselli, K., Lieberburg, I., and Kagan, B. L. (1994) *Biochem. Biophys. Res. Commun. 202*, 1142−1148.
12. Müller, W. E., Koch, S., Eckert, A., Hartmann, H., and Scheuer, K. (1995) *Brain Res. 674*, 133−136.
13. Gibson Wood, W., Eckert, G. P., Igbavboa, U., and Müller, W. E. (2003) *Biochim. Biophys. Acta 1610*, 281−290.
14. Walter, M. F., Mason, P. E., and Mason, R. P. (1997) *Biochem. Biophys. Res. Commun. 233*, 760−764.
15. Del Mar Martinez-Senac, M., Villalain, J., and Gomez-Fernandez, J. C. (1999) *Eur. J. Biochem. 265*, 744−753.
16. McLaurin, J., and Chakrabartty, A. (1996) *J. Biol. Chem. 271*, 26482−26489.
17. McLaurin, J., and Chakrabartty, A. (1997) *Eur. J. Biochem. 245*, 355−363.
18. Terzi, E., Holzemann, G., and Seelig, J. (1994) *Biochemistry 33*, 7434−7441.
19. Mason, R. P., Estermyer, J. D., Kelly, J. F., and Mason, P. E. (1996) *Biochem. Biophys. Res. Commun. 222*, 78−82.
20. Mason, R. P., Jacob, R. F., Walter, M. F., Mason, P. E., Avdulov, N. A., Chochina, S. V., Igbavboa, U., and Wood, W. G. (1999) *J. Biol. Chem. 274*, 18801−18807.
21. Dante, S., Hauss, T., and Dencher, N. A. (2002) *Biophys. J 83*, 2610−2616.
22. Hauss, T., Grzesiek, S., Otto, H., Westerhausen, J., and Heyn, M. P. (1990) *Biochemistry 29*, 4904−4913.
23. Bradshaw, J. P., Davies, S. M., and Hauss, T. (1998) *Biophys. J. 75*, 889−895.
24. Jao, S. M. K., Talafous, J., Orlando, R., and Zagorski, M. G. (1997) *Amyloid: Int. J. Exp. Clin. Invest. 4*, 240−244.
25. Franks, N. P., and Lieb, W. R. (1979) *J. Mol. Biol. 133*, 469−500.
26. King, G. I., and White, S. H. (1986) *Biophys. J. 49*, 1047−1054.
27. Darkes, M. J., and Bradshaw, J. P. (2000) *Acta Crystallogr. D 56* (Part 1), 48−54.
28. Yip, C. M., Darabie, A. A., and McLaurin, J. (2002) *J. Mol. Biol. 318*, 97−107.
29. Yip, C. M., and McLaurin, J. (2001) *Biophys. J. 80*, 1359−1371.
30. Kohno, T., Kobayashi, K., Maeda, T., Sato, K., and Takashima, A. (1996) *Biochemistry 35*, 16094−16104.
31. Hunt, J. F., Earnest, T. N., Bousche, O., Kalghatgi, K., Reilly, K., Horvath, C., Rothschild, K. J., and Engelman, D. M. (1997) *Biochemistry 36*, 15156−15176.
32. Hunt, J. F., Rath, P., Rothschild, K. J., and Engelman, D. M. (1997) *Biochemistry 36*, 15177−15192.
33. Soekarjo, M., Eisenhawer, M., Kuhn, A., and Vogel, H. (1996) *Biochemistry 35*, 1232−1241.
34. Moll, T. S., and Thompson, T. E. (1994) *Biochemistry 33*, 15469−15482.
35. White, S. H., and Wimley, W. C. (1998) *Biochim. Biophys. Acta 1376*, 339−352.
36. Thorgeirsson, T. E., Russell, C. J., King, D. S., and Shin, Y. K. (1996) *Biochemistry 35*, 1803−1809.
37. Arispe, N., Pollard, H. B., and Rojas, E. (1996) *Proc. Natl. Acad. Sci. U.S.A. 93*, 1710−1715.

BI035056V